VOL. 17, NO. 9, MAY 2022 ISSN 1819-6608
ARPN Journal of Engineering and Applied Sciences

www.arpnjournals.com

MODELLING AND SIMULATION OF AN ADSORPTION PROCESS USING ACTIVATED CARBON FROM COCONUT SHELLS

Edward Samuel Efretuei, Idowu Iyabo Olateju, John Olusoji Owolabi and Abdulwahab Giwa
Department of Chemical and Petroleum Engineering, College of Engineering, Afe Babalola University, Ado-Ekiti, Ekiti State, Nigeria
E-Mail: edwardefretuei@yahoo.com

ABSTRACT

In this work, modelling and simulation of a vacuum swing adsorption unit has been carried out using Aspen Adsorption simulator. The major chemical components involved in the development of the model were carbon dioxide and nitrogen. Peng-Robinson equation of state was chosen as the fluid package. The model of the system was developed by inserting the necessary blocks and streams into the flowsheet, connecting the blocks with the streams, inputting the stream parameters and specifying the kinetic models as well as the mass transfer coefficients required for the simulation. In the simulation environment,0.09-0.1kmol/s of dry flue gas was passed through a 2-bed adsorption system in a six-step cycle and the adsorbent used was Acticarb GC1200, which was activated carbon derived from coconut shells. The adsorbent beds used were designed to have values that would give maximum efficiency of the system. The model developed for the system was run for 10 cycles. The results obtained showed that the unit could be operated with two adsorber beds each having a diameter of 1.76479 m and a height of 3.53568 m with an isentropic vacuum pump. It was also discovered that the adsorbent employed for the simulation was able to capture CO_2 from flue gas under the established performance criteria. The results obtained were found to compare well with those of other researches. It is recommended that the process should be subjected to optimisation for the purpose of improvement in the design and operation.

Keywords: vacuum swing adsorption, aspen adsorption, dry flue gas, purity, productivity.

1. INTRODUCTION

Adsorption is a surface phenomenon where adsorbent is a substance that adheres to another substance on its surface. A substance which accumulates on the surface of an adsorbent is named adsorbate. Adsorption might be a chemical or physical process, or combination of those, which occurs at the common boundary of two phases, such as liquid-solid, gas-solid, gas-liquid or liquid-liquid. In other words, adsorption is a change in concentration of a certain substance (i.e., contaminant) at an interface where an initial concentration is decreased. Historically, adsorption has been first observed by C.W. Scheele in 1773 for gases. Lowitz has continued observation of experiments in 1785 for solutions. Currently, adsorption is actively studied by many institutes around the world (Musin, 2013).

Adsorption has importance for industries that work with gas, petroleum, air and water purification. It is applied for purifications of organics and SO_2 from gas phase. Also, water can be extracted from O_2, CH_4, N_2.In addition, NO_x can be separated from N_2. Adsorption is also used for gas separations, such as N_2 from O_2, acetone and C_2H_2 from vent stream, and CO, CH_4, CO_2, N_2, and Ar from hydrogen. In the liquid phase, adsorption is applied, for example, for organic and inorganic removal, and decolourization (Musin, 2013).

Adsorption plays an important role in many fields and facilitates multifarious applications in chemical and industrial processes, e.g., separation of mixtures, purification of air, water and wastewater, industrial catalytic process, heterogeneous catalysis, purification and drying of chemical substances, colour removal in sugar processing, refining of vegetable oils, recovery of useful materials from industrial waste, separation of metal ores and adsorption of toxic gases in the gas mask, etc. The adsorption phenomenon occurs at all interfaces. However, the solid-liquid interface has found greater applications in many electrochemical, chemical, and biological processes. One of the materials that can be used to accomplish adsorption is activated carbon (Efretuei, 2020).

Activated carbon (AC) is a valuable engineering material for water treatment and material refining. It has wide acceptance for use because of its relative cheapness and universal adsorptive capacity for majority of impurities over other adsorbents such as silica gel and molecular sieves. Despite its wide use and ready source of raw materials for its production, it is imported by most major industries, in particular, from Europe and Asian countries such as Thailand and Malaysia. The high demand, especially from the growing packaged water industries (PWIs) that produce treated water in plastic sachets or bottles has led to the presentation of ordinary charred materials as activated carbon to unsuspecting buyers. This is because there are no ready methods for the determination of the quality, except in few companies such as the beverage and liquor industries, which mostly receive supplies directly from foreign sources. Literature is replete with studies showing that activated carbon can easily be manufactured from carbonaceous wastes such as palm kernel shells (PKS), coconut shells, corn cobs and stalks, bagasse wastes, and most other agricultural and livestock wastes. What is critical to each raw material used as matrix is the carbonization and activation conditions for the production and the medium for such processing (Adewumi, 2009).

Adsorption is an essential process to many chemical industries for reasons varying from product purification to waste water treatment to refinery operation. Activated carbon, being one of the oldest adsorbents, finds its use in a lot of industries for purposes such as water

treatment to carbon capture, however even though it is highly utilized means of acquiring it locally are not numerous and means of acquiring it from renewable resources close to local industries, so as to be cost effective are even less prevalent. As a result of this, means by which its usage may be made more efficient and overall process may be optimized for activated carbon from natural sources such as coconut shells are underdeveloped (Efretuei, 2020).

This research work has been carried out to simulate a vacuum swing adsorber used in the adsorption capture of CO_2 using activated carbon from coconut shells as the adsorbent. The work was done for the purpose of promoting feasibility of activated carbon produced from local natural sources as adsorbent in target industries.

2. METHODOLOGY

2.1 Modelling and Simulation

Simulation is of a general CO_2 recovery from dry flue gas process using a vacuum pressure swing adsorber (VPSA) with one stage. Although, there exist quite a number of simulation software available, because of Aspen adsorptions ability to specifically manipulate the adsorption process based on chosen data for the various equipment such as the adsorption vessels and valves, as well as change data gotten based on adsorption kinetics and models used, Aspen Adsorption (Aspen, 2019) was chosen for simulation in this work.

The step-by-step approach employed for the development and simulation of the adsorption model in this work are as outlined below.

a) A new blank simulation was opened (see Figure-1), and the chemical components of concern were added as a component set from the aspen properties interface (Figure-2).

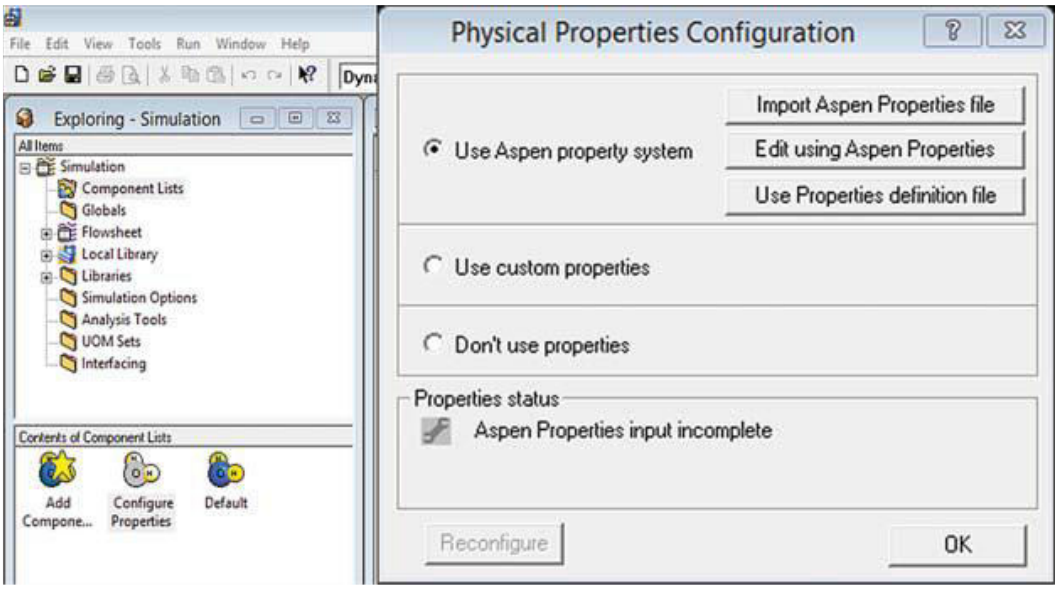

Figure-1. Physical properties configuration tab of a simulation.

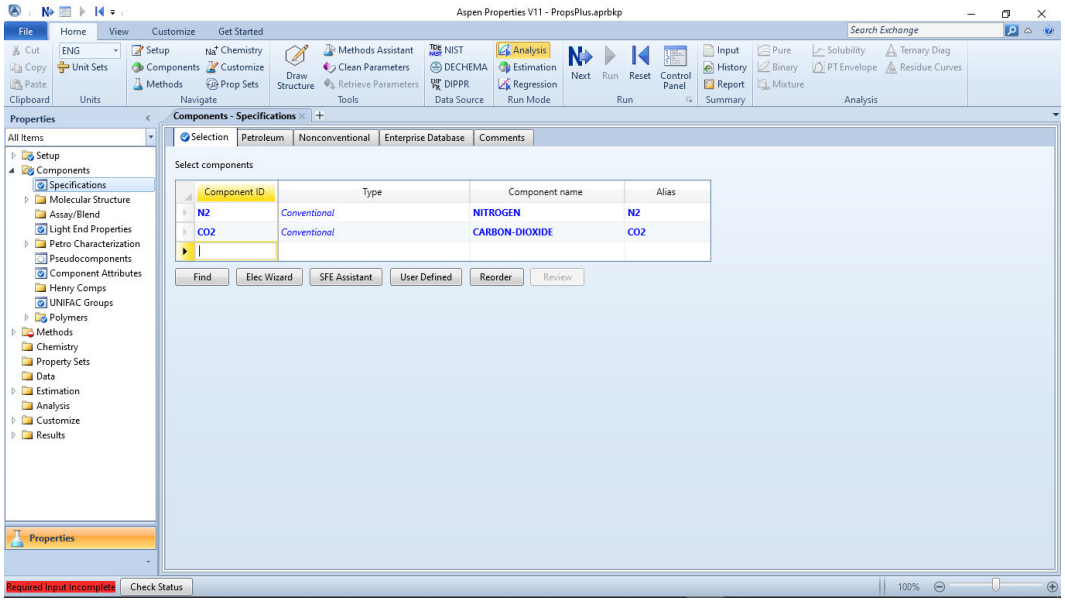

Figure-2. Aspen properties window for component selection.

b) As the components were added in the aspen properties interface, Peng-Robinson equation of state was also selected as the base method to calculate the thermodynamic properties (Figure-3).

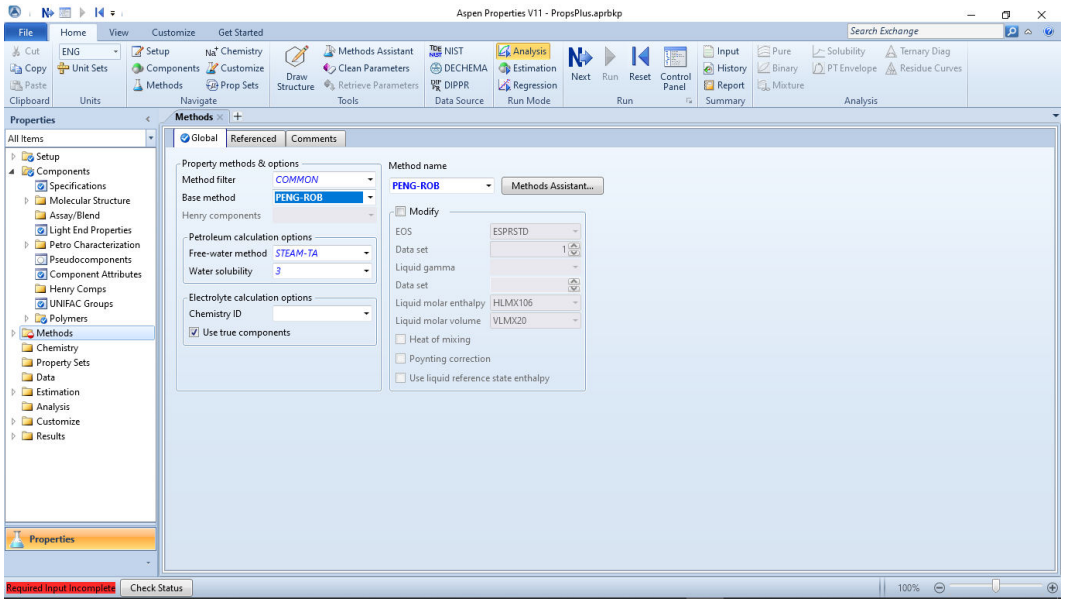

Figure-Fehler! Kein Text mit angegebener Formatvorlage im Dokument.**.** Aspen properties window for thermodynamic properties estimation method selection.

c) The necessary block and streams were then put into the flowsheet (Figure-4). Such blocks in Aspen Adsorption include: gas tank blocks, feed and product blocks, adsorber beds, gas valves and the gas material connections, or streams which connect the blocks.

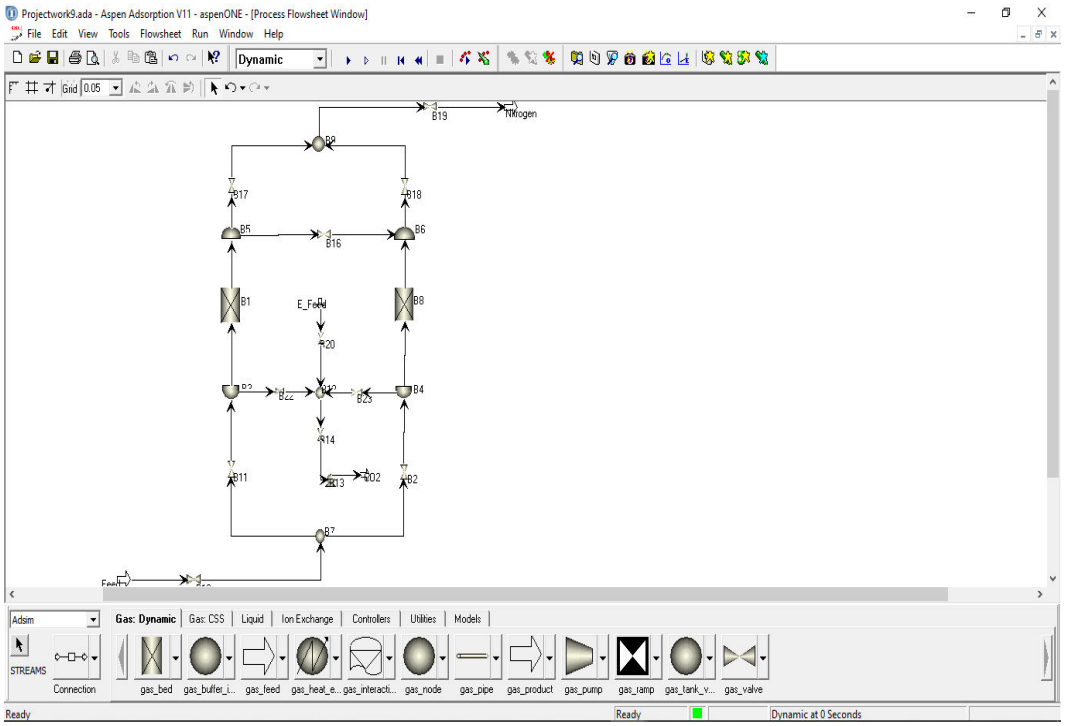

Figure-4. Aspen adsorption flowsheet.

d) The operating conditions were specified thus:

- Through the default form for the process models in the flow sheet, the operating conditions with which the simulation was to be carried out could be inputted and edited. Adsorber specification involved selection of one vertical adsorber bed, with no heat exchanger within the adsorbent layer (Figure-5).

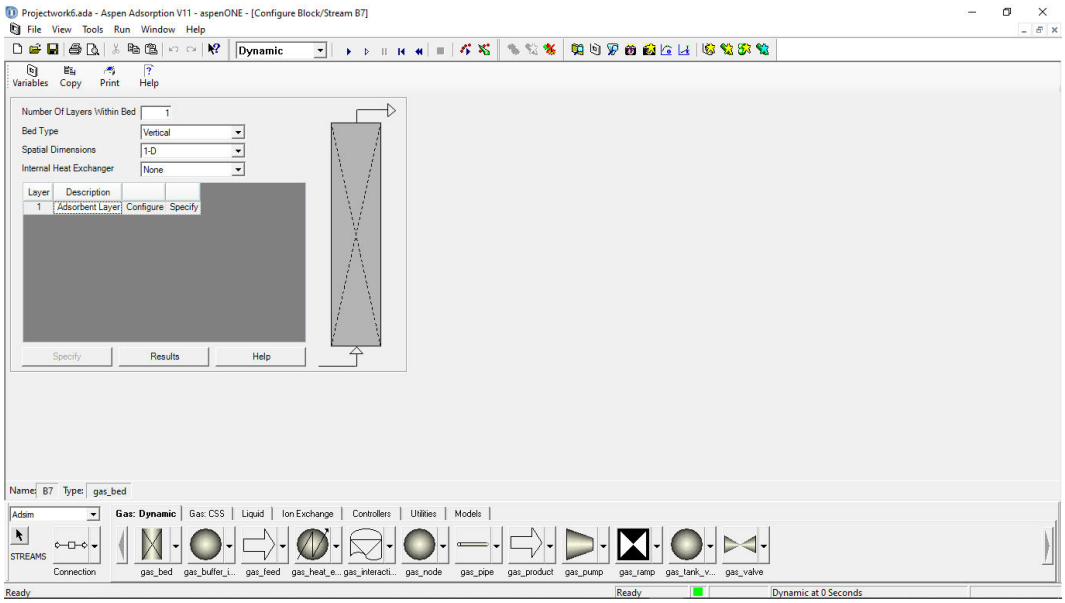

Figure-5. Adsorber bed general window.

- The gas model assumption for the dynamic Vacuum Pressure Swing Adsorber (VPSA) model concerned was selected as the upwind differencing scheme 1(UDS1); see Figure-6.

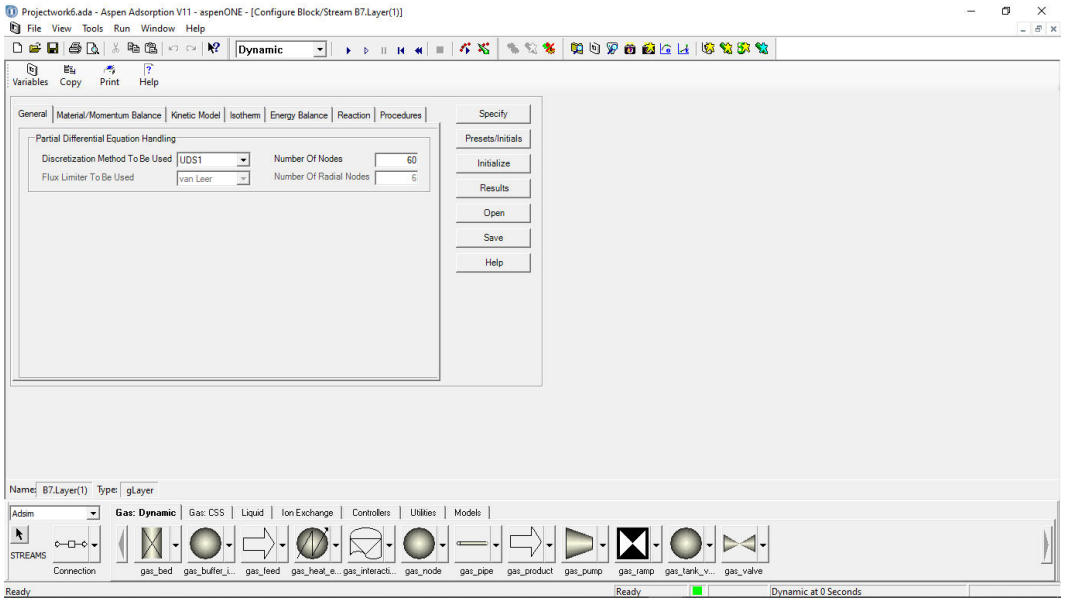

Figure-6. Adsorber bed configuration window.

- Convection only was chosen for the Material Balance Assumption. Ergun Equation, which was found to be valid for both laminar and turbulent flows, was selected for the Momentum Balance Assumption. See Figure-7.

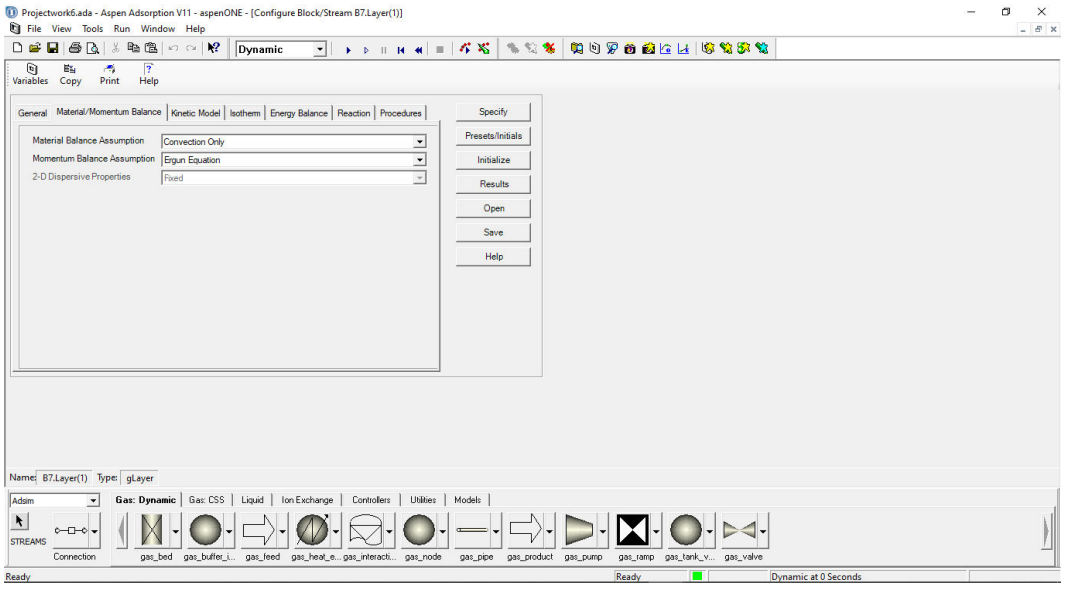

Figure-7. Configuration window material/momentum balance tab.

- Thereafter, Kinetic Model Assumption and Mass Transfer Coefficients were specified (Figure-8). In this case, Linear Driving Force (LDF) assumption was chosen in the Kinetic Model Assumption box, meaning the mass transfer resistances were lumped as a single overall factor while Mass Transfer Coefficient for each component was taken as constant throughout the bed.

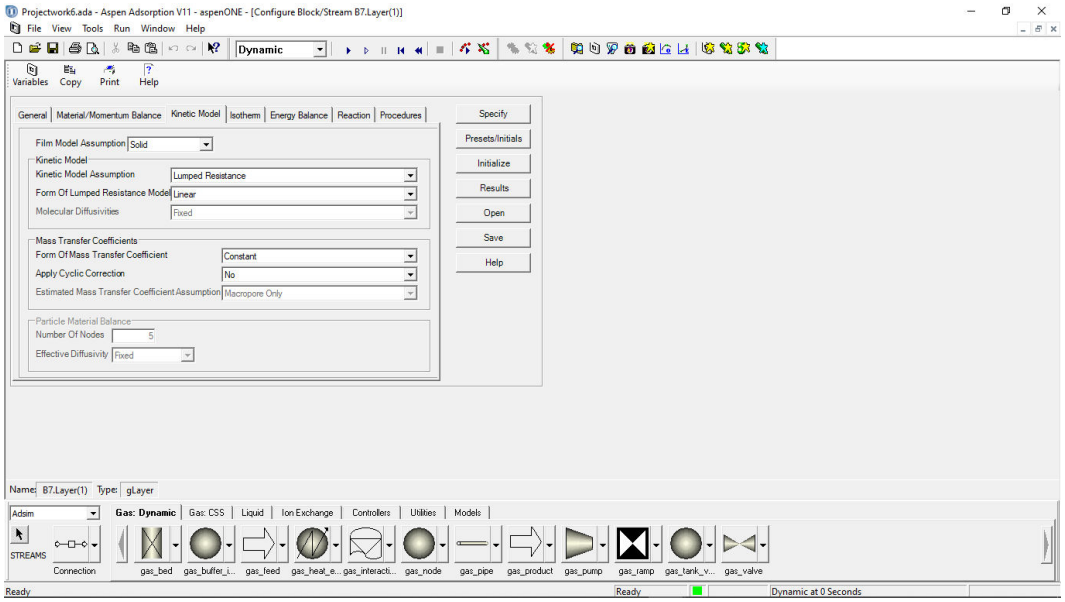

Figure-8. Configuration window kinetic model tab.

- For the specification of Isotherm Assumption, Dual Site Langmuir Isotherm was used as the isotherm model, which was discovered to be a function of partial pressure in the system (Figure-9).

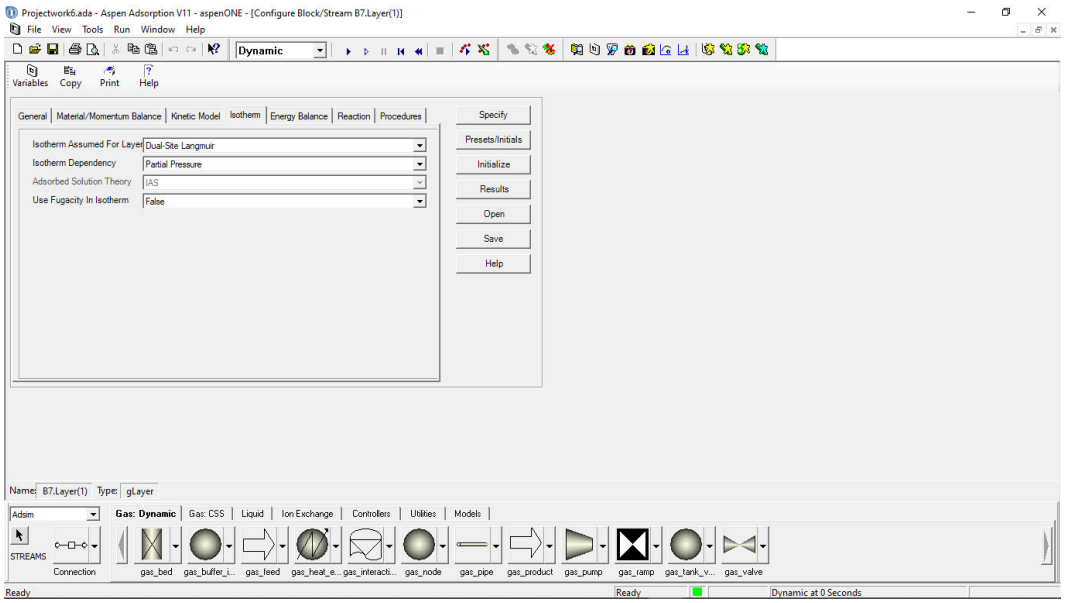

Figure-9. Configuration window isotherm tab.

- Regarding the Energy Balance Specification, isothermal was used as the energy assumption, and the beds were assumed to be adiabatic, as shown in Figure-10. The reason for this was because of the long cycle time and negligible rise in temperature that were assumed (Chen *et al.*, 2017).

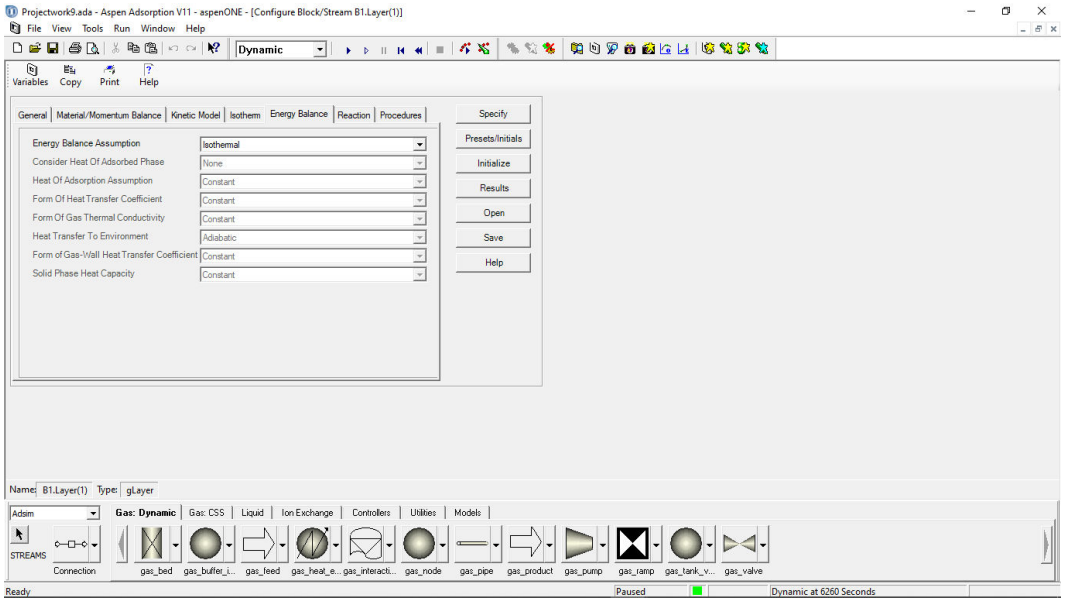

Figure-10. Configuration window energy balance tab.

- It was taken that no reaction was occurring in the VPSA system.
- After all the assumptions were defined, Adsorbent Bed Data Table was considered and the required specifications needed in the adsorbent layer data table were entered as shown in Figure-11.

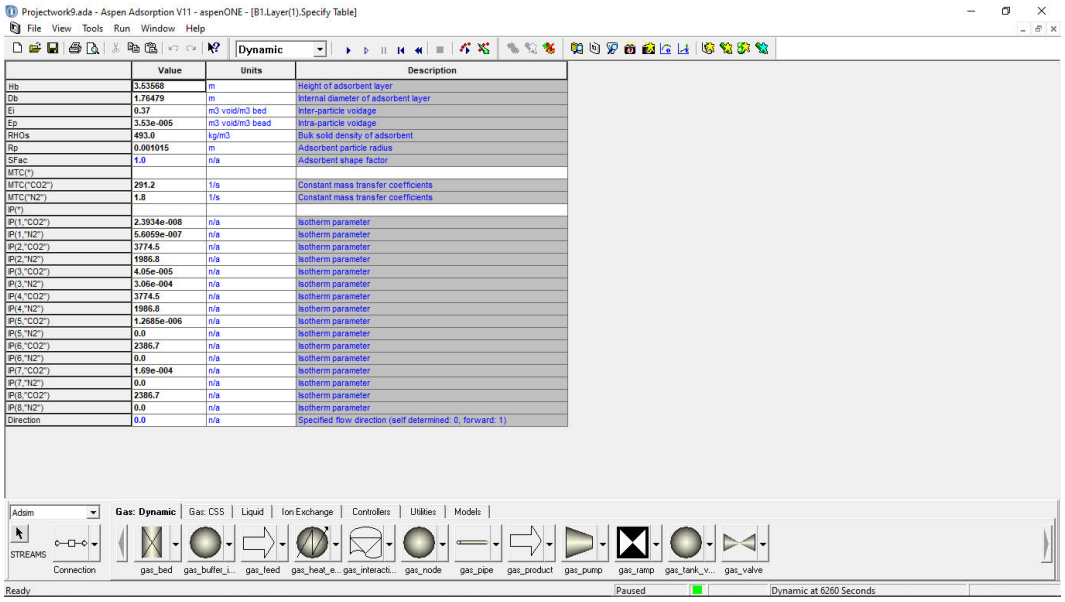

Figure-11. Adsorber Bed specification window.

e) The initial conditions were set as outlined below (Figure-12):

- The initial condition of the beds, as well as the feed and product blocks need were set by taking the ratio of Nitrogen to Carbon dioxide to be 0.85:015, and the temperature of both the gas phase and solid phase as 20^{o}C.
- Feed composition in the feed block was fixed with 0.85 mole fraction for nitrogen and 0.15 for carbon dioxide. Temperature and pressure in the feed were fixed at 20^{o}C and 1.5bar, respectively. For the product block, pressure was set to 0.5 bar and 1 bar, while concentration and temperature were the same as with the feed block.

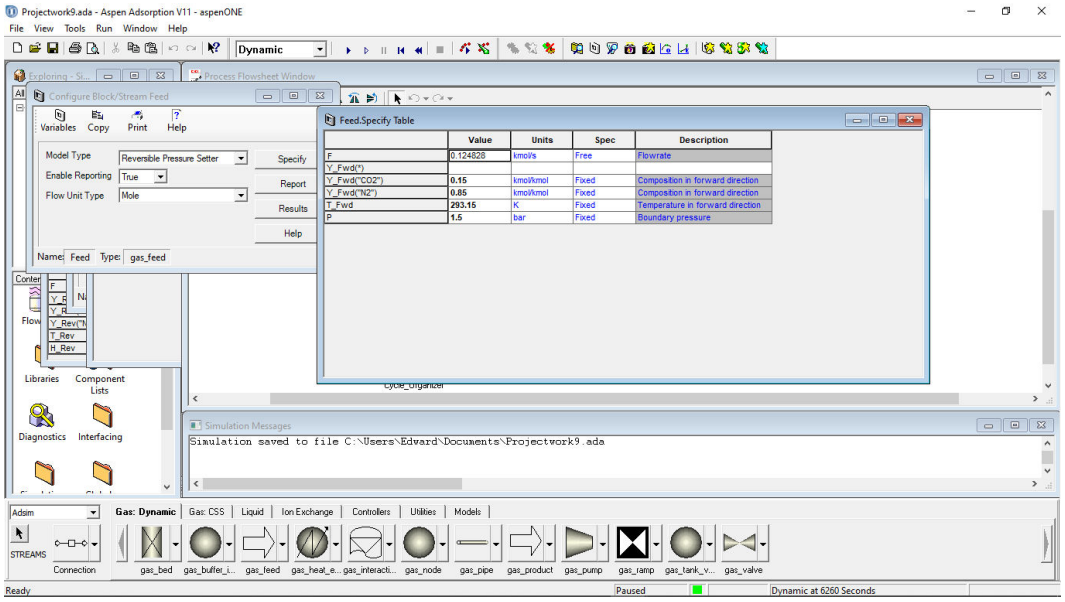

Figure-12. Feed specification table.

f) The flowsheet was initialized, and this applied the initial condition set in the previous step to all the nodes of the adsorber beds. At this stage, all the gas beds were set to have uniform composition.

g) In order to carry out the event scheduling with cycle organizer and valve setting, the dynamic valve opening and closing necessary to simulate the VPSA process was set up and controlled through a cycle organizer inserted in the simulation. Also, the valve coefficient (Cv) values of the valves, which were acting as flow setters for the simulation were specified. The Cycle Organizer was added through the Tools buttons, after which the steps which dictated how the model would be run were specified. Refer to Figure-13.

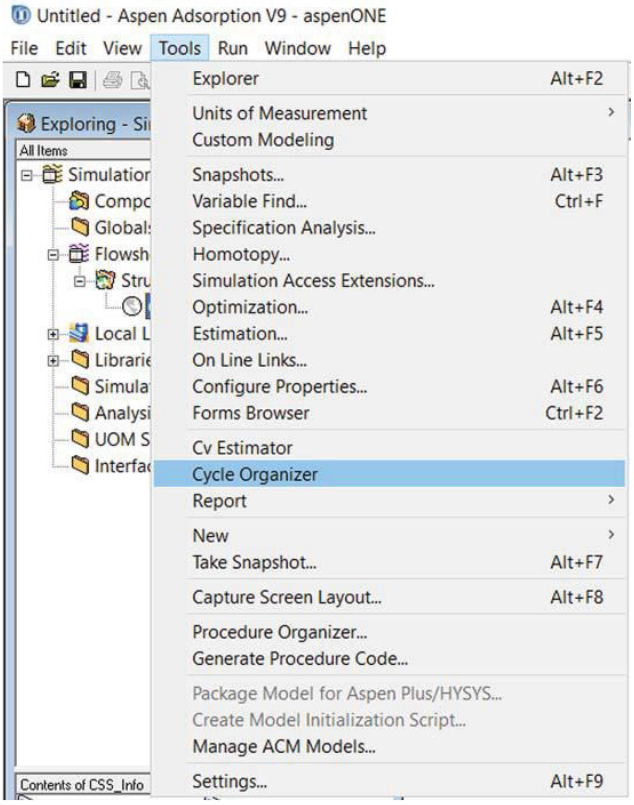

Figure-13. Toolbar for cycle organizer.

- **Step 1:** Adsorption in bed 1 and purge of bed 2 were carried out, and this was set to run for 300s. From the Manipulated window of the step, the opened and closed valves during the step were added and defined (see Figure-14).

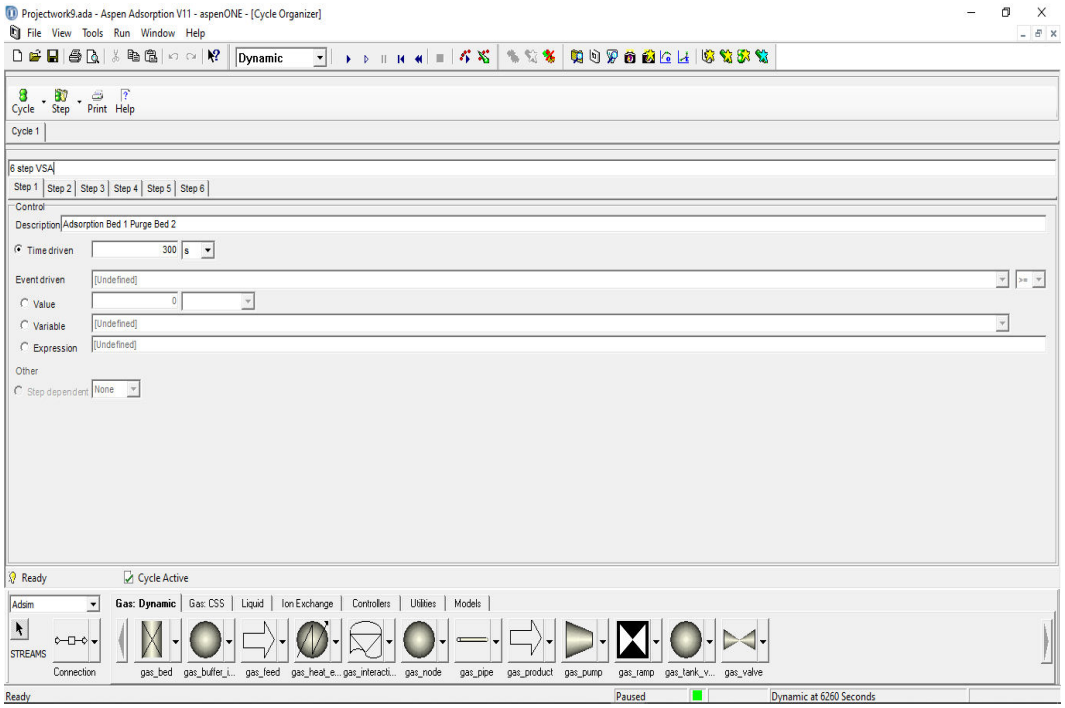

Figure-14. Step 1 of Vacuum Swing Adsorbercycle.

- **Step 2:** Pressure equalization between the two beds in the model was carried out. In this case, the low-pressure bed was brought up to a high pressure enough for the next step to take place. The step was event-controlled to end as soon as the required pressure was reached Figure-15.

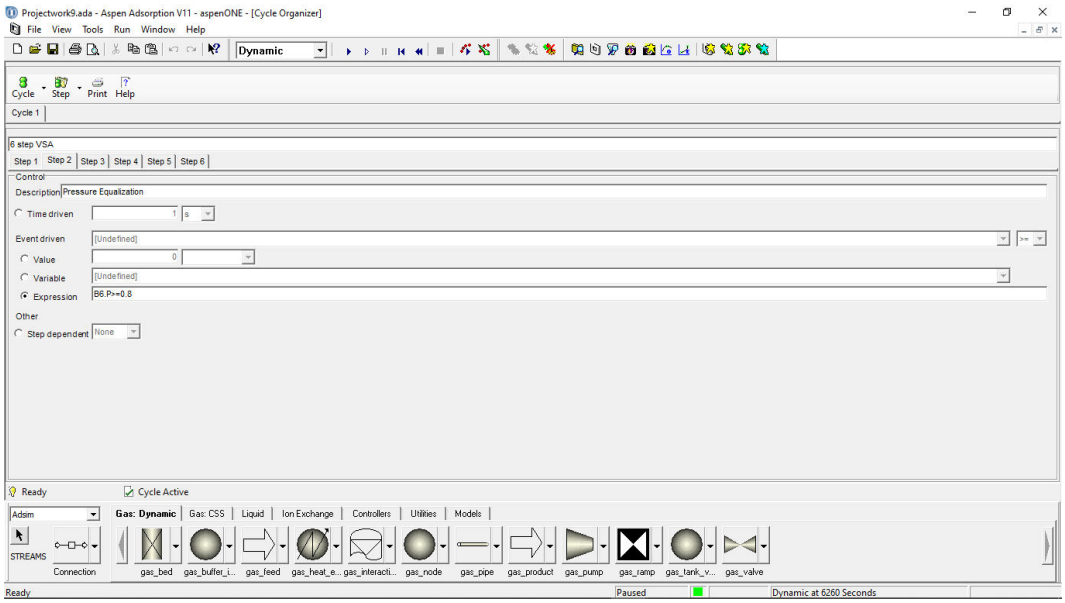

Figure-15. Step 2 of Vacuum Swing Adsorber cycle.

- **Step 3:** At this stage, the blowdown of bed 1 and pressurization of bed 2 were carried out. This step was an event-controlled one that would end as soon as the pressure defined in the controlling expression was reached. Bed 2 was set to be pressurized to greater than 1 bar, while bed was set to be depressurized to less than 0.6 bar (Figure-16).

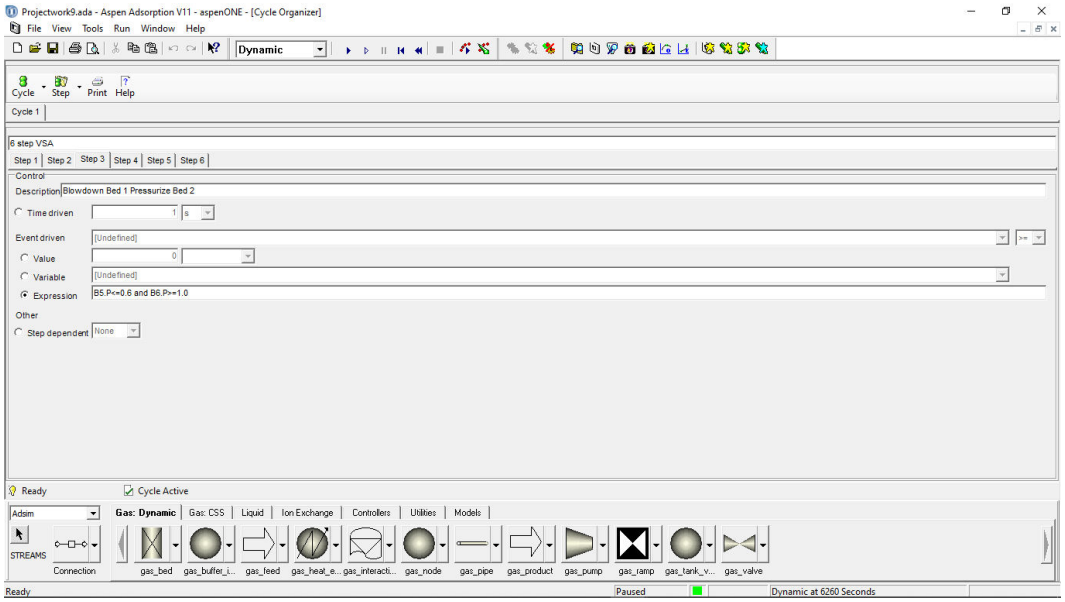

Figure-16. Step 3 of Vacuum Swing Adsorber cycle.

- Steps 4, 5 and 6 were mirrors of steps 1, 2 and 3. As such, they had reversed controlling expressions.

Having defined all the necessary steps, the maximum number of cycles of the simulation was set as 10 to give an end point. At this point and the Cycle Organizer was generated and activated before running the simulation (Figure-17).

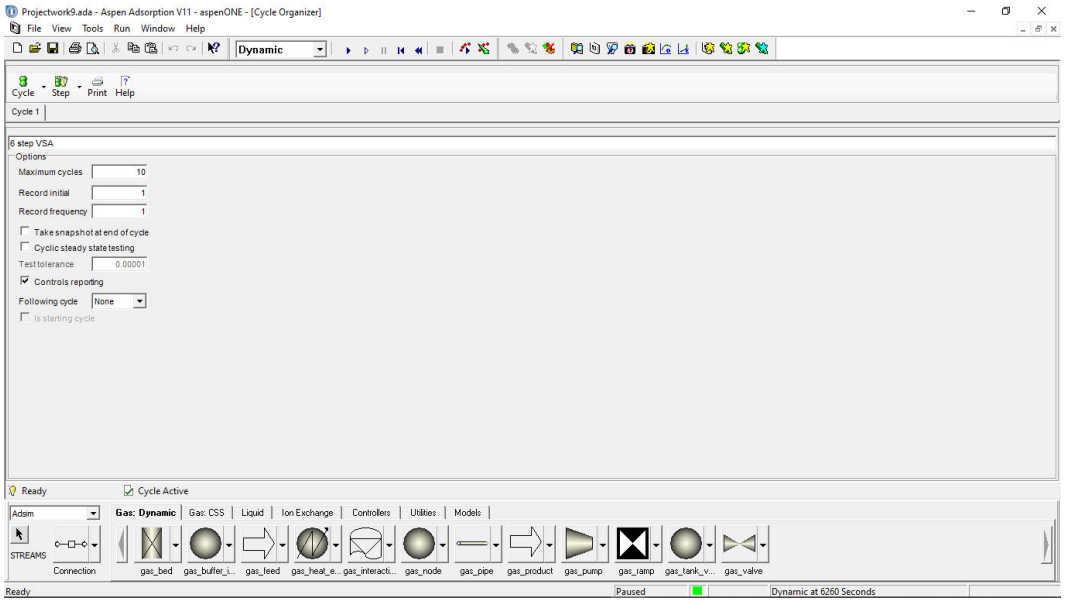

Figure-17. Vacuum Swing Adsorber cycle option.

3. RESULTS AND DISCUSSIONS

The results obtained from the simulation of the model developed for the capture of CO_2 using vacuum swing adsorption process are given and discussed in terms of performance criteria, viz. product purity, productivity and recovery, as outlined thus.

The dynamic 2-bed vacuum swing adsorption model was run for 10 cycles and reached steady state after one cycle. This could be attributed to the assumptions made on instant equilibrium. From the results of the model under assumed pressure for adsorption and desorption pressure, average purity of CO_2 in CO_2 product stream was shown to be about 30%. To put this in context, there was the need to compare the results to other setups for CO_2 capture. From the research work of Liu *et al.* (2011), comparisons were made on CO_2 capture and storage employing both one-stage and two-stage setups using zeolite as the adsorbent. In the work, ranges for purity were shown to be between 40% to 77% for the one stage setups. It was also mentioned that purity could overall be brought up to above 50% by employing heavy product rinse, but this would result in a decrease in productivity.

As such, this method was not implemented. As the adsorbent used, Zeolite 13X, was of greater capacity under similar operating conditions to the model used here, the reason for showing greater purity was understandable. Comparing to setups that used activated carbon such as in the work of Shen *et al.* (2012) that used activated carbon beads, it was shown that Vacuum Pressure Swing Adsorber (VPSA) setups could range in purity from 30% to 60% (Shen *et al.*, 2012; Liu *et al.*, 2011).

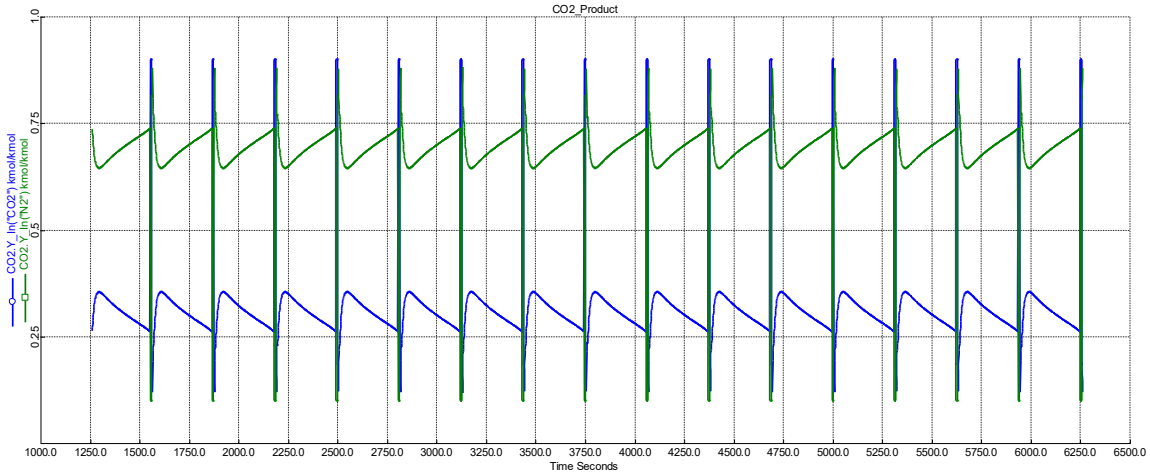

Figure-18. Graph of CO_2 and N_2 composition in product stream over time from steady state.

In terms of the overall cycle, the model developed was also characterised by overall short pressure equalisation and blowdown times of about 5 and 9 seconds. From the literature, it was discovered that blowdown times and pressure equalisation times were short and have effects on periods of higher purity. This characteristic of increased purity was also reflected in the developed model as can be seen by the spikes in captured CO_2 composition indicated by the blue peaks in Figure-18.

Figure-19 shows how bed capacity for adsorbed CO_2 was changing over time in the two adsorber beds for the model. In terms of productivity, for the 10-cycle period, $0.1202 kmol CO_2/(kg_{ads} h)$ was generated. Comparing this to the results obtained from other simulations done with zeolite and activated carbon beads as contained in the researches of Liu *et al.* (2011) and Shen *et al.* (2012), model productivity was quite low owing to lower working capacity of model, which was further caused by higher desorption pressure used for model (P_{desorb}=0.5 bar). Working capacity of model was found to swing between $1.86 mol/kg_{ads}$ - $1.07 mol/ kg_{ads}$, and this was in agreement with the observation in the work of Shen*et al.* (2012).

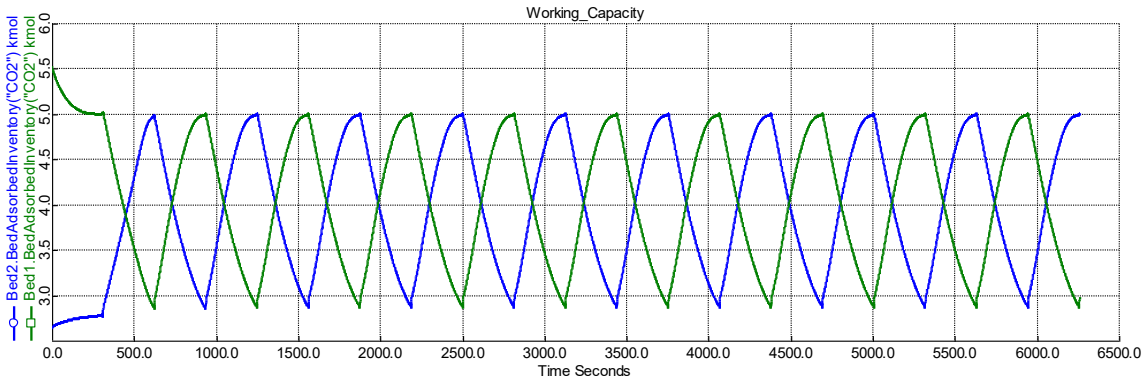

Figure-19. Adsorber bed capacity of Beds 1 and 2 over 10 cycles.

Projectwork9.ada - Aspen Adsorption V11 - aspenONE - [CO2.Report Table]

File View Tools Run Window Help

Dynamic

	Value	Units	Description
Total_Material	181.613	kmol	Total material received at boundary
Total_Component(*)			
Total_Component("CO2")	56.19	kmol	Total component received at boundary
Total_Component("N2")	125.423	kmol	Total component received at boundary
Avg_Composition(*)			
Avg_Composition("CO2")	0.309394	kmol/kmol	Average composition received at boundary
Avg_Composition("N2")	0.690606	kmol/kmol	Average composition received at boundary
Total_Energy	-21702.0	MJ	Total energy received at boundary
Cycle_Total_Material	18.2893	kmol	Total received at boundary over last cycle
Cycle_Total_Component(*)			
Cycle_Total_Component("CO2")	5.77141	kmol	Total component received at boundary over last cy
Cycle_Total_Component("N2")	12.5179	kmol	Total component received at boundary over last cy
Cycle_Avg_Composition(*)			
Cycle_Avg_Composition("CO2")	0.315562	kmol/kmol	Average composition received at boundary over la
Cycle_Avg_Composition("N2")	0.684438	kmol/kmol	Average composition received at boundary over la
Cycle_Total_Energy	-2230.43	MJ	Total energy received at boundary over last cycle

Figure-20. CO_2streamreport table showing total CO_2 received.

Projectwork9.ada - Aspen Adsorption V11 - aspenONE - [Feed.Report Table]

File View Tools Run Window Help

Dynamic

	Value	Units	Description
Total_Material_Fwd	602.381	kmol	Total material fed at boundary
Total_Component_Fwd(*)			
Total_Component_Fwd("CO2")	90.3572	kmol	Total component fed at boundary
Total_Component_Fwd("N2")	512.024	kmol	Total component fed at boundary
Avg_Composition_Fwd(*)			
Avg_Composition_Fwd("CO2")	0.15	kmol/kmol	Average composition fed at boundary
Avg_Composition_Fwd("N2")	0.85	kmol/kmol	Average composition fed at boundary
Total_Energy_Fwd	-35658.3	MJ	Total energy fed at boundary
Total_Material_Rev	0.0	kmol	Total material received at boundary
Total_Component_Rev(*)			
Total_Component_Rev("CO2")	0.0	kmol	Total component received at boundary
Total_Component_Rev("N2")	0.0	kmol	Total component received at boundary
Avg_Composition_Rev(*)			
Avg_Composition_Rev("CO2")	0.0	kmol/kmol	Average composition received at boundary
Avg_Composition_Rev("N2")	0.0	kmol/kmol	Average composition received at boundary
Total_Energy_Rev	0.0	MJ	Total energy received at boundary
Cycle_Total_Material_Fwd	60.3277	kmol	Total material fed at boundary over last cycle
Cycle_Total_Component_Fwd(*)			
Cycle_Total_Component_Fwd("CO2")	9.04916	kmol	Total component fed at boundary over last cycle
Cycle_Total_Component_Fwd("N2")	51.2785	kmol	Total component fed at boundary over last cycle
Cycle_Avg_Composition_Fwd(*)			
Cycle_Avg_Composition_Fwd("CO2")	0.15	kmol/kmol	Average composition fed at boundary over last cycl
Cycle_Avg_Composition_Fwd("N2")	0.85	kmol/kmol	Average composition fed at boundary over last cycl
Cycle_Total_Energy_Fwd	-3571.13	MJ	Total energy fed at boundary over last cycle
Cycle_Total_Material_Rev	0.0	kmol	Total material received at boundary over last cycle
Cycle_Total_Component_Rev(*)			
Cycle_Total_Component_Rev("CO2")	0.0	kmol	Total component received at boundary over last cycl
Cycle_Total_Component_Rev("N2")	0.0	kmol	Total component received at boundary over last cycl
Cycle_Avg_Composition_Rev(*)			
Cycle_Avg_Composition_Rev("CO2")	0.0	kmol/kmol	Average composition received at boundary over last
Cycle_Avg_Composition_Rev("N2")	0.0	kmol/kmol	Average composition received at boundary over last
Cycle_Total_Energy_Rev	0.0	MJ	Total energy received at boundary over last cycle

Figure-21. Feed stream report table.

Referring to the results given in Figures 20 and 21, using total CO_2 received in as feed and total CO_2 going out at CO_2 stream, the recovery was calculated, as the percentage molar ratio of CO_2 out to that of CO_2 in, to be 62.18%. Compared to the percentage recovery from the work of Shen *et al.* (2012), in which the recovery for 1-stage or two bed setups were said to range from 60% to over 80%, the results obtained in this work was found to fall within an established recovery range.

Furthermore, the results obtained from the changes in composition along the bed profile during the various steps are given as in Figures 22-24.

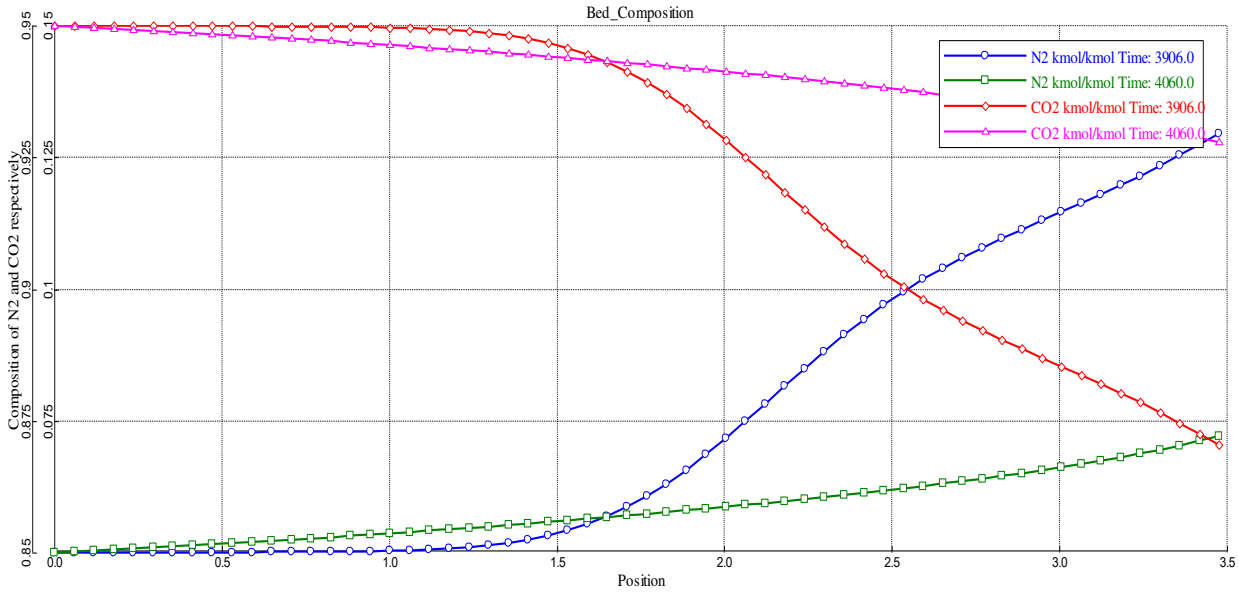

Figure-22. Compositional change down bed 1 for cycle 7 Steps 1 and 2.

Figure-22 shows how CO_2 and N_2 composition change down the length of the adsorber Bed 1 during adsorption and pressure equalization. CO_2 concentration at the top of the bed for step 1and Step 2 were seen to be the same as the bed was still being fed flue gas of the same composition in both steps. However, going down the bed, a sharp drop was seen in the CO_2 composition of Bed 1 in step one, but a more gradual decline for CO_2 was foundin Step 2. This could be attributed to the fact that, as breakthrough had already occurred in the previous step, most of the bed was already in equilibrium and more CO_2 could not be adsorbed. Similar characteristics were also shown by nitrogen, but in a different way as nitrogen composition in both steps started out the same way but the composition of Step 1 rapidly increased while only a gradual increase was observed in that of Step 2.

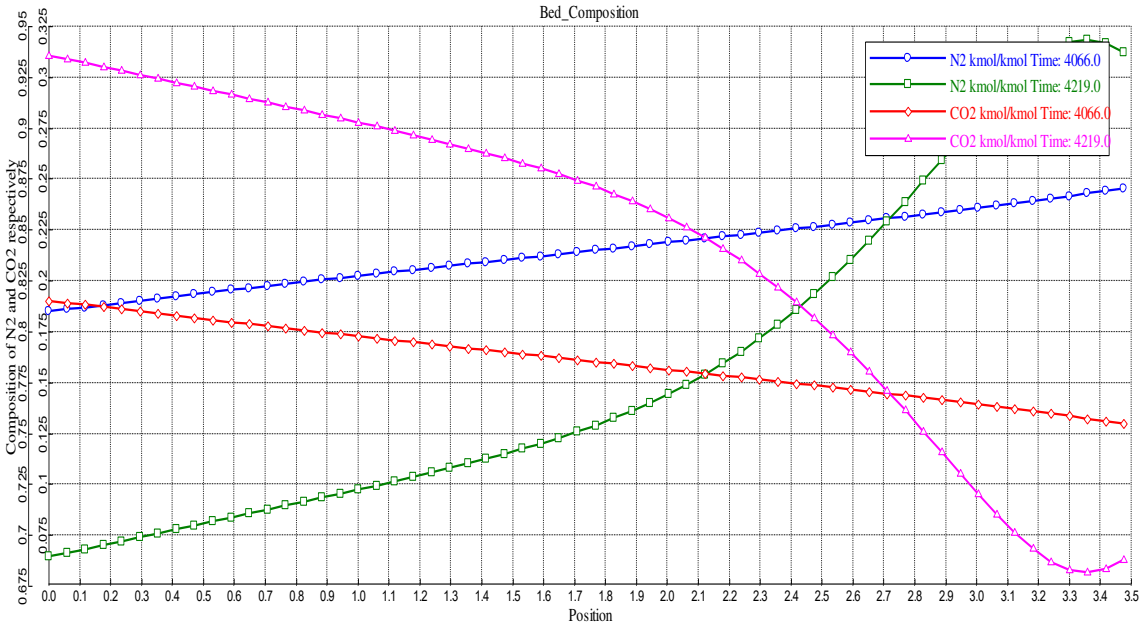

Figure-23. Compositional change down bed 1 cycle 7 for Steps 3 and 4.

In Steps 3 and 4, relatively high values for CO_2, with composition in Step 3 reducing almost linearly, whereas composition in step 4 going down drastically. This could be explained that, as in Step 3, although $CO_2$was just beginning to be desorbed from the bed, the pressure for such to be carried out as fast as possible had not been reached. Once again, the reverse was true for N_2 compositions that started out relatively low but increase linearly for Step 3 and quite rapidly for Step 4.

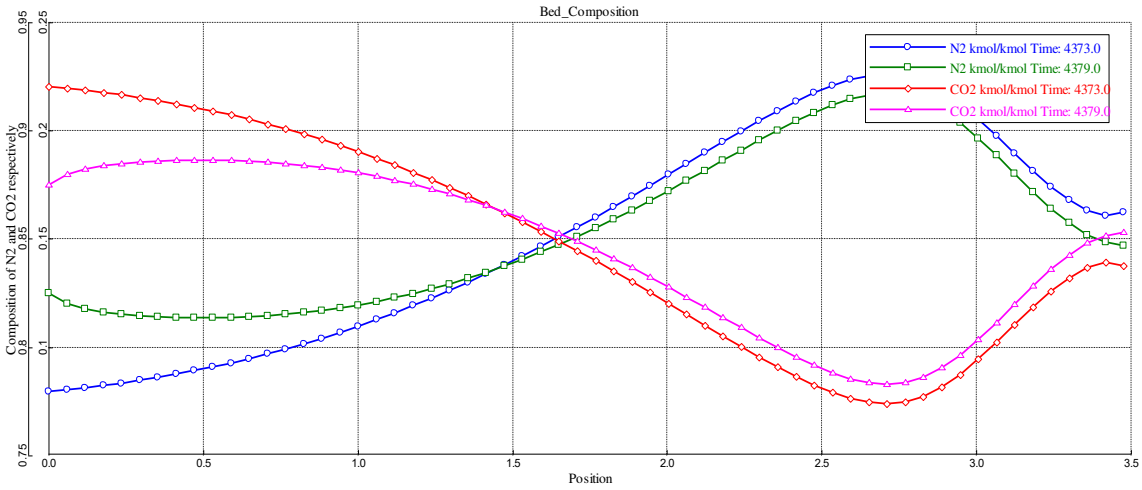

Figure-24. Compositional changes down bed 1 cycle 7 Steps 5 and 6.

As can be seen in Figure-24, during the Steps 5 and 6, where pressure equalization and repressurization took place for bed 1, CO_2 composition was found to vary widely down the bed with composition in Step 5 being slightly higher for CO_2 as purge had just been carried out. A slight dip in composition was just observed in Step 6, and this could be attributed to how quickly the step operations were carried out. Down the bed, there was an overall higher concentration of N_2 in both steps.

4. CONCLUSIONS

The results obtained from the simulation of the model developed for a vacuum pressure swing adsorption unit using two adsorber beds with the aid of Aspen Adsorption revealed that the equipment could be operated with two adsorber beds each having a diameter of 1.76479m and a height of 3.53568m with an isentropic vacuum pump. Also, it was shown from the results that the adsorbent employed for the simulation, which was activated carbon from coconut shells, was able to capture CO_2 from flue gas under the established performance

criteria, although process employed still needs to be optimized and improved.

ACKNOWLEDGMENT

Special appreciation goes to Ambassador Aare Afe Babalola, LL.B, FFPA, FNIALS, FCIArb, LL.D, SAN, OFR, CON - The Founder and President, and the Management of Afe Babalola University, Ado-Ekiti, Ekiti State, Nigeria for providing a very conducive environment that enabled the accomplishment of this research work.

REFERENCES

[1] Adewumi I. K. 2009. Activated Carbon for Water Treatment in Nigeria: Problems and Prospects. In: Yanful, E. K. (ed.) Appropriate Technologies for Environmental Protection in the Developing World, pp. 115-122. Springer, New York.

[2] Aspen. 2019. Aspen Adsorption V11 (37.0.0.395). Aspen Technology, USA.

[3] Chen E., Rolin K. and Stillman Z. 2017. Activated Carbon Based Carbon Dioxide Process. Senior Design Reports. University of Pennsylvania Scholarly Commons. 1-191.

[4] Shen C., Liu Z., Li P. and Yu J. 2012. Two-Stage VPSA Process for CO_2 Capture from Flue Gas Using Activated Carbon Beads. Industrial & Engineering Chemistry Research. 51(13): 5011-5021.

[5] Efretuei E. S. 2020. Modeling and Simulation of an Adsorption Process Using Activated Carbon from Coconut Shells. B.Eng. Project Report Submitted to Afe Babalola University, Ado-Ekiti, Ekiti State, Nigeria.

[6] Musin E. 2013. Adsoprtion Modelling. Bachelor's thesis on Environmental Engineering Submitted to Mikelli University of Applied Sciences, Mikkeli, Finland.

[7] Liu Z., Grande C. A., Li P., Yu J., Rodrigues A. E. 2011. Multi-bed Vacuum Pressure Swing Adsorption for Carbon Dioxide Capture from Flue Gas. Separation and Purification Technology. 81, 307-317.